RESEARCH ARTICLE

Asymmetric adaptation with functional advantage in human sensorimotor control

John J. Jeka · Kelvin S. Oie · Tim Kiemel

Abstract Human movement control is inherently stochastic, requiring continuous estimation of self-motion based upon noisy sensory inputs. The nervous system must determine which sensory signals are relevant on a time scale that enables successful behavior. In human stance control, failure to effectively adapt to changing sensory contexts could lead to injurious falls. Nonlinear changes in postural sway amplitude in response to changes in sensory environmental motion have indicated a dynamic changing of the weighting of the nervous system's multiple sensory inputs so that estimates are based upon the most relevant and accurate information available. However, the time scale of these changes is virtually unknown. Results here show systematic changes in postural gain when visual scene motion amplitude is increased or decreased abruptly, consistent with sensory re-weighting. However, this re-weighting displayed a temporal asymmetry. When visual motion increased, gain decreased within 5 s to a value near its asymptotic value. In contrast, when visual motion decreased, it took an additional 5 s for gain to increase by a similar absolute amount. Suddenly increasing visual motion amplitude threatens balance if gain remains high, and rapid down-weighting of the sensory signal is required to avoid falling. By contrast, slow up-weighting suggests a conservative CNS strategy. It may not be functional to rapidly up-weight with transient changes in the sensory environment. Only sustained changes necessitate the slower up-weighting process. Such results add to our understanding of adaptive processing, identifying a temporal asymmetry in sensory re-weighting dynamics that could be a general property of adaptive estimation in the nervous system.

Keywords Sensory re-weighting · Multisensory fusion · Vision · Adaptive control · Posture

Introduction

A crucial component of flexible upright stance control is the multiple sensory modalities that are sensitive to different forms of physical energy and are fused to provide information about self-motion relative to the motion in the environment. The multisensory fusion process necessitates that our nervous systems estimate which sensory signals are relevant within a given sensory context. How this multisensory integration is accomplished has been the focus of several recent theoretical efforts (e.g., Anastasio and Patton 2004; Knill and Pouget 2004; Pouget 2006; Ernst and Banks 2002), which have argued that neural computation can be understood as probabilistic (i.e., Bayesian) in nature: because neural systems are inherently noisy, their sensory inputs cannot be strictly deterministic. It is postulated that neurons compute the conditional

J. J. Jeka (✉) · K. S. Oie · T. Kiemel
Department of Kinesiology, University of Maryland,
College Park, MD, USA
e-mail: jjeka@umd.edu

J. J. Jeka · K. S. Oie
Neuroscience and Cognitive Sciences Program,
University of Maryland, College Park, MD, USA

J. J. Jeka
Bioengineering Graduate Program, University of Maryland,
College Park, MD, USA

K. S. Oie
U.S. Army Research Laboratory,
Human Research and Engineering Directorate,
Aberdeen Proving Ground, 21005 Aberdeen, MD, USA

probability of the stimulus value (e.g., if a target is present or not within a neuron's receptive field), given the uncertainty in their sensory inputs (cf., Anastasio and Patton 2004, for an in-depth treatment of the Bayes' rule model to multisensory neurons in the deep superior colliculus).

The Bayesian framework can also be applied to the problem of estimating quantities that change stochastically with time, such as when sensory estimates of self-motion need to be continuously updated for compensatory corrections to an individual's motor state (Todorov 2004; Wolpert and Ghahramani 2000). In the case of a linear stochastic system, Bayesian inference can be implemented using a Kalman filter. Kalman filters have been used, for example, in models of postural control of human upright stance (van der Kooij et al. 1999; Kiemel et al. 2002; Kuo 2005). In these models, a Kalman filter continually estimates the body's position and velocity based on noisy inputs from multiple senses, and these estimates are used to generate appropriate motor commands to stabilize upright stance.

Visual, somatosensory, and vestibular inputs, all play important roles in postural control (Bronstein et al. 1990; Horak and Macpherson 1996; Jeka et al. 2000). Systematic spatiotemporal patterns of postural sway responses can be induced by visual and somatosensory environmental motion (Dijkstra et al. 1994; Jeka et al. 1998, 2000). For example, an increase in the amplitude of environmental motion is accompanied by a corresponding decrease in the amplitude of compensatory sway in response to environmental motion (i.e., gain) (Oie et al. 2001, 2002; Peterka 2002; Peterka and Benolken 1995). One of the prevailing hypotheses is that this nonlinear aspect of postural responses indicates that the nervous system adapts to changing sensory contexts by decreasing its dependence, or weighting, when information from one or more sensory systems is compromised, while increasing its weighting of other inputs in order to prevent a loss of balance (e.g., Carver et al. 2005; Keshner et al. 2004; Mahboobin et al. 2005; Oie et al. 2002; van der Kooij et al. 2001; however, see Mergner et al. 2003 for an alternative interpretation).

For a complete description of the re-weighting process, its magnitude and time course are necessary. Recent evidence suggests that sensory re-weighting may be intact, for example, in the elderly (Allison et al. 2006), but at a slower time scale that prevents appropriate postural responses (Allison et al. 2005). Previous studies have implicated deficient multisensory re-weighting as a contributor to instability and falls in older adults (Teasdale et al. 1991a, 1991b, 1993; Hay et al. 1996). Multisensory re-weighting is thought to be slowed in older adults, both in circumstances where sensory information is withdrawn or becomes unreliable, and when reliable sensory information

becomes available after a period of withdrawal. For example, Woollacott et al. (1986) observed appropriate responses in young control subjects on the first trial in different sensory organization test (SOT) conditions, but it was not until the second trial that many elderly subjects responded appropriately. While indicative of deficient processing between trials, effects are difficult to assess in a temporally precise manner.

Moreover, recent accounts of human postural control use an adaptive Kalman filter to model the multisensory re-weighting process (van der Kooij et al. 2001; Carver et al. 2006). By an adaptive Kalman filter, we mean a state estimator that has the form of a Kalman filter with one or more parameters that are varied based on some adaptive scheme. Different models hypothesize different adaptive schemes; however, currently there exist little experimental data to constrain the type of adaptive scheme implemented. In the Carver model, adaptation is based on minimizing the mean squared ankle torque specified by the neural controller. As a consequence of this adaptation scheme, the model predicts what we refer to as a "temporal asymmetry" in response to changes in environmental motion (Carver et al. 2006). Specifically, if the amplitude of environmental motion is changed abruptly, the initial decrease in gain when environmental motion is increased is predicted to be faster than the initial increase in gain when environmental motion is decreased. This finding was completely unexpected and was not designed into the model in any explicit manner. In the present experiment, we tested this prediction by analyzing the dynamics of re-weighting when visual amplitude changed within a trial. Results are qualitatively consistent with the asymmetric prediction of the Carver et al. model.

Methods

Thirty participants (15 female, 15 male, mean age 20.9 (±1.6) years of age) took part in this study. All participants had normal or corrected-to-normal vision, were free of any self-reported musculoskeletal or neurological disorders, and gave written consent to participate according to the guidelines implemented by the Internal Review Board of the University of Maryland.

Participants were asked to stand quietly, approximately 0.5 m from a large translucent screen (2.0 m × 1.0 m, Da-Lite Screen Company, Inc., Warsaw, IN), as shown in Fig. 1. The visual stimulus consisted of a pattern of randomly positioned, white triangles distributed throughout a fronto-parallel plane on a black background. When the visual scene was stationary, all triangles were of equal size (approximately 0.2° × 0.3° × 0.2° of visual angle). The pattern was rear-projected onto the screen via a direct drive
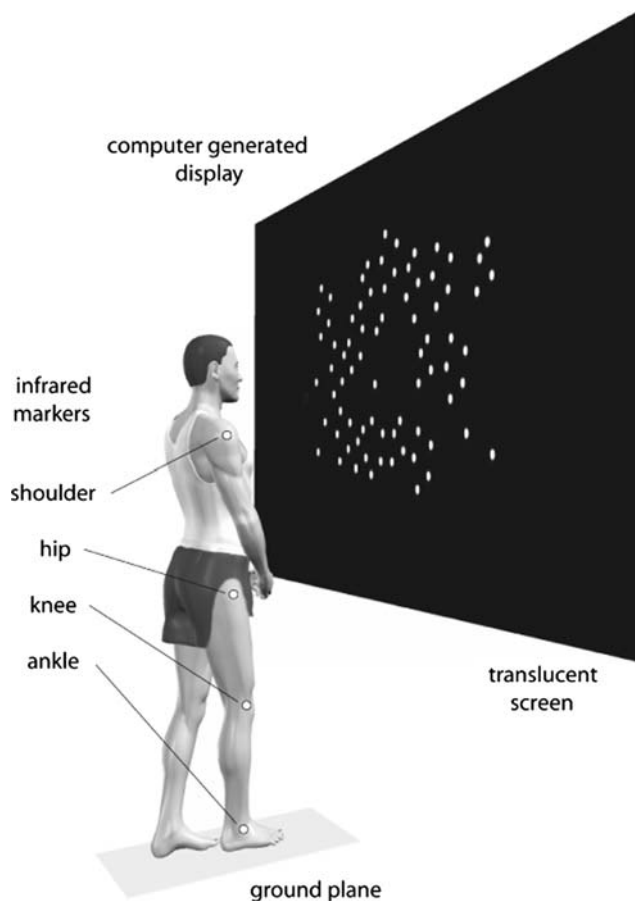
Fig. 1 Experimental setup showing the subject standing in a semi-tandem stance in front of the computer-generated visual display

image light amplifier (D-ILA) projector (JVC M15, JVC America, Wayne, NJ). The visual displays were generated using a desktop PC (Dell PWS650, Dell, Inc., Austin, TX) with a Wildcat4 7210 video adapter (3Dlabs US, Madison, AL) at a resolution of 1,280 × 1,024 pixels.

Before the beginning of a trial, the visual scene was stationary, providing binocular information about the distance to the visual wall. Sinusoidal environmental motion was then specified by varying the projected size and the distance between the triangles to simulate translation in a forward–backward direction of the entire visual scene relative to the participant, with the mean position of the simulated wall corresponding to the position of the projection screen (0.5 m from the subject). The focus of expansion of visual motion was positioned at the approximate center of the participant's foveal region prior to the start of data collection, and no triangles were placed near the focus of expansion to suppress the visibility of aliasing effects. Participants wore goggles that limited their visual field to approximately 100° vertically and 120° horizontally, while allowing them to wear prescription eyeglasses, if necessary. The goggles prevented subjects from seeing

the edges of the screen or other potential visual cues relative to stance control.

Participants were asked to keep their head level, eyes open, gaze directed at the focus of expansion, and to avoid locking their knees during the conduct of an experimental trial. Stimulus motion comprised a 0.4 Hz sinusoid whose amplitude was changed twice within a 360 s trial, from 0.3 to 1.2 cm and back to 0.3 cm at 120 and 180 s into the trial, respectively. A stimulus frequency of 0.4 Hz was chosen for the strong postural responses documented between 0.2 and 0.4 Hz (e.g., Kiemel et al. 2006). Choosing the higher end of this range improved the temporal resolution of the dynamic response on a cycle-to-cycle basis. Stimulus amplitudes of 0.3 and 1.2 cm are known to produce strong and weak postural responses, respectively (Kiemel et al. 2006), allowing for the re-weighting process to be studied dynamically. Three trials were run for all participants.

Participants' postural responses to visual display motion were captured using an OptoTrak camera position tracking system (Northern Digital, Inc., Waterloo, ON, CA) at a sampling rate of 60 Hz. Markers were placed at the heel (posterior calcaneous), ankle (lateral malleolus), knee (lateral tibial tuberosity), hip (greater trochanter), and shoulder (acromion) on the right side of the body. Center-of-mass (COM) trajectories were estimated using a three-segment model based upon the trajectories of these markers (cf. Winter 1991).

To characterize the postural response to visual scene motion, we used the frequency response function (FRF) (Bendat and Piersol 2000) from visual scene position to COM position at the stimulus frequency. To achieve reasonable temporal resolution along with an accurate estimate of the power spectrum density, each trial was divided into 72.5-s intervals (two stimulus cycles per interval). The complex-valued FRF for each interval was computed by subtracting the mean from the COM trajectory, multiplying the stimulus and COM trajectories by a Hamming window to reduce side-lobe leakage of power from non-stimulus frequencies, computing Fourier transforms, and then dividing the COM Fourier transform by the stimulus Fourier transform. The absolute value of the FRF is gain; the postural response amplitude is divided by the stimulus amplitude. The argument of the FRF is phase, which indicates the temporal relationship between postural response and stimulus motion. A positive phase indicates that COM position leads stimulus position. Our use of gain to track changes in coupling strength to the stimulus is subject to errors due to transients. In the Appendix we use simulated data to show that these errors are expected to be small.

Figure 2a shows an example of FRFs from individual subjects for one time interval. Because these FRFs were
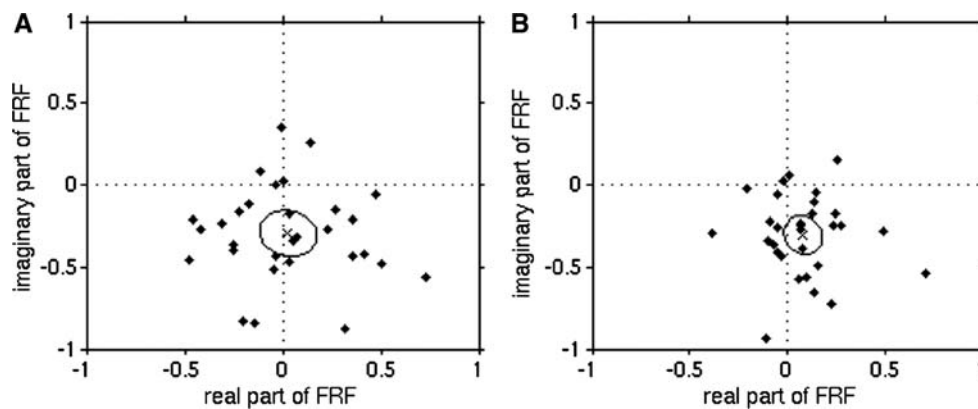
Fig. 2 FRFs at the stimulus frequency (0.4 Hz) from individual subjects for last 5-s time interval before first switch (time interval b1). **a** Directly computed FRFs. **b** FRFs estimated from linear regression. Mean FRF is indicated by *times symbol*. The absolute value (distance from the origin) and argument (phase angle in the complex plane) of

the mean FRF are the group gain and phase values, respectively, used to characterize the average responses of the subjects (see Fig. 5 below). Ellipse indicates boundary of 95% confidence region for mean FRF

estimated based on a limited amount of data (one 5-s interval from three trials), the FRF estimates contained large sampling errors. Although using linear regression reduced the sampling errors (Fig. 2b), the distribution of FRFs still included the origin in the complex plane. To reduce the effect of sampling errors on our analysis, rather than computing gains and phases for individual subjects, we averaged FRFs across subjects (the 'x' symbols in Fig. 2) and computed "group gain" and "group phase" as the absolute value and argument, respectively, of the average FRF (see Appendix).

Our statistical analysis was based on estimated FRFs from five 5-s time intervals (see Figs. 4, 5). These intervals were: immediately before the first switch (b1), immediately after the first switch (a1), immediately before the second switch (b2), immediately after the second switch (a2), and at the end of the trial (e). FRFs for intervals a1 and a2, which occurred during fast changes in the FRFs following a switch, were estimated directly only from the data from their respective time intervals. FRFs for intervals b1, b2, and e occurred just before a change in visual stimulus amplitude or at the end of the trial (see Fig. 5), with previous time periods during which visual stimulus amplitude was constant. To improve the estimate of these FRFs, we assumed that the time interval previous to b1, b2, and e was linear in the complex plane. Specifically, we fit the FRFs by a linear function of the time-interval index over three separate periods: the 18 5-s time intervals before the first switch, the six time intervals before the second switch, and the 30 time intervals before the end of the trial. We used the fitted FRF value for the 18.5, 6 and 30 s time intervals as the estimated FRF for the time intervals b1, b2 or e, respectively. To insure that we were characterizing these FRFs over relatively stable periods of behavior, the time periods for the linear regressions exclude the first six time

intervals (30 s) at the beginning of the trial and after each visual amplitude switch during which changes in the FRFs were clearly nonlinear. We fit the FRFs by computing least-squares fits of their real and imaginary parts.

We tested various null hypotheses concerning group gains from the time intervals b1, a1, b2, a2, and e, where linear regression was used to obtain better estimates for the intervals b1, b2, and e. Tests were performed using a statistical model that assumed multivariate normality for the real and imaginary parts of the FRFs. For each null hypothesis, group gains and phases for the constrained model (the statistical model with parameters constrained by the null hypothesis) and unconstrained model were estimated using the method of maximum likelihood, and the likelihood ratio was tested using the same method and degrees of freedom applied to the Wilks' Λ in linear regression (Seber 1984). For group gain, we made comparisons for all pairs of the time intervals b1, a1, b2, a2, and e. To test for temporal asymmetry, we tested whether the changes at the two switches summed to zero (i.e., H_0: $(g_{b1} - g_{a1}) + (g_{b2} - g_{a2}) = 0$). Group phases were tested in the same fashion. A closed testing procedure (Hochberg and Tamhane 1987) was used to adjust p-values to control the family-wise Type I error rate at 0.05 for tests on gains, and separately for the tests on phase. The preceding tests on gain represent our primary analysis of re-weighting in this study. We also tested several additional linear contrasts involving gain to further refine our characterization of re-weighting (see Results). For these additional tests, we report unadjusted p-values.

In addition to FRFs, position and velocity variability of the residual sway response was computed as the standard deviation of COM motion excluding the postural response at the stimulus frequency (cf., Jeka et al. 2000). Higher variability reflects lower postural stability. Variability was

calculated over longer segments (six 60 s segments in a trial) than gain and phase because we were interested in whether visual amplitude changes led to changes in overall postural stability, rather than cycle-to-cycle effects. The Fourier transform for each 60 s segment was computed at the stimulus frequency and then inverse transformed to compute the sway response only at the stimulus frequency. This component was subtracted from the original COM position trajectory, resulting in the corresponding residual COM position trajectory. The residual COM velocity trajectory was computed by finite differences with a time step of 0.167 s, to reduce the effect of experimental measurement noise on the velocity computation. Position or velocity variability was then computed as the standard deviation of the respective residual trajectory. We tested for differences in the log of position and velocity variability using Hotelling's T^2 statistic. A closed testing procedure (Hochberg and Tamhane 1987) was used to control the family-wise Type I error rate at $\alpha = 0.05$ separately for position and velocity variability.

Results

Figure 3 presents an exemplar time series of COM (Fig. 3a) and stimulus (Fig. 3b) position for a single trial. To visualize more clearly the spatiotemporal relationship between the postural response and the sinusoidal stimulus motion, the slow component of postural motion (cf., Kiemel et al. 2006) was removed by applying a zero-phase, 0.1 Hz high-pass Butterworth filter (Fig. 3c). Figure 3d shows a close up view of the filtered COM position superimposed on stimulus position around the first switch from low to high stimulus amplitude.

Gain and phase

Figure 4 shows exemplars of the mean cycle-to-cycle gain and phase for two different subjects (A–C and D–F, respectively). In general, subjects exhibited similar qualitative changes in response to the changes in stimulus motion amplitude: gain decreased relatively quickly when stimulus amplitude was increased at 120 s in the trial, and increased more slowly when stimulus amplitude was then decreased at 180 s. Individual differences were observed in the overall response to stimulus motion. For example, gain to low amplitude stimulus motion was relatively higher for the subject in Fig. 4a than for the subject in Fig. 4d. These individual differences are largely responsible for the inter-subject variability shown in the mean cycle-to-cycle gain and phase collapsed across all 30 subjects presented in Fig. 5.
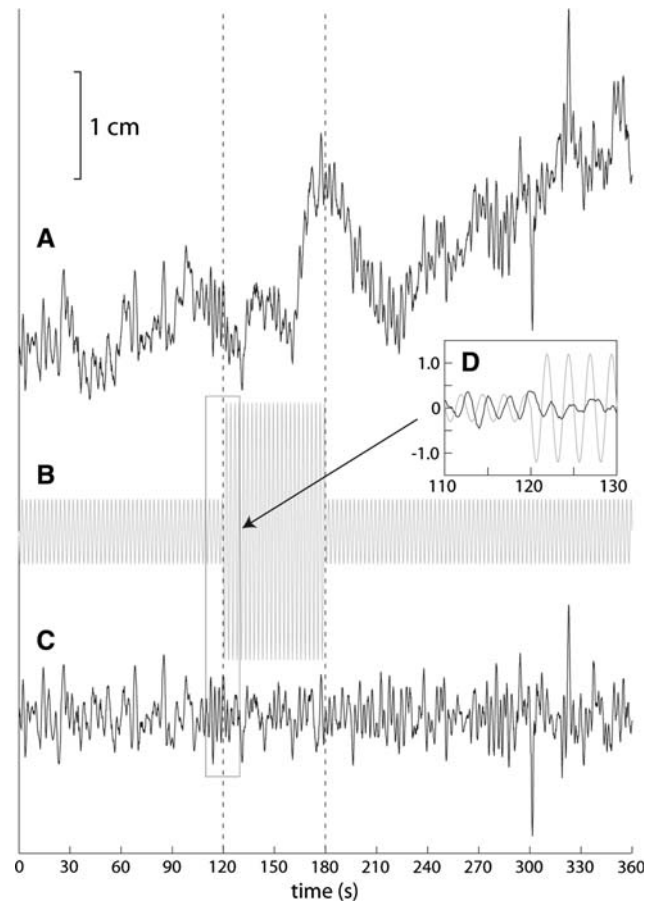

Fig. 3 Exemplar time series of COM position (*bold lines* in *A*, *C*, *D*) and stimulus position (*thin lines* in *B*, *D*). *A* Raw COM position, *B* stimulus position, *C* high-pass (0.1 Hz) filtered COM position, and *D* COM and stimulus position at first stimulus amplitude switch

Across subjects, when visual motion amplitude was low ($t \leq 120$ s, $t \geq 180$ s), gain was observed to be higher than when visual motion amplitude was high (120 s $< t < 180$ s), with phase showing an approximately constant phase of about $-90°$. This general pattern was observed across all subjects, though the more variable mean gains across subjects at the beginning of trials (~ 10–50 s) is due to the large observed variability in phase during this time period.

Gain based on the average FRF across subjects varied significantly across the five time intervals $b1$, $a1$, $b2$, $a2$, and e ($p < 0.001$). There were no significant differences in phase ($p = 0.707$). Pair-wise contrasts for gain revealed significant differences between the estimated FRFs: $g_{b1} > g_{b2}$ ($p < 0.001$) and $g_{b2} < g_e$ ($p < 0.001$), and no difference between g_{b1} and g_e ($p = 0.652$). This result reproduces the characteristic gain-dependence of the postural response upon the amplitude of visual motion, where gain has been observed to be higher when stimulus amplitude was low, and lower when stimulus amplitude

Fig. 4 Mean cycle-to-cycle gain and phase for two individual subjects (*A–C, D–F*). Mean gain and phase are based on estimated FRFs averaged across three trials
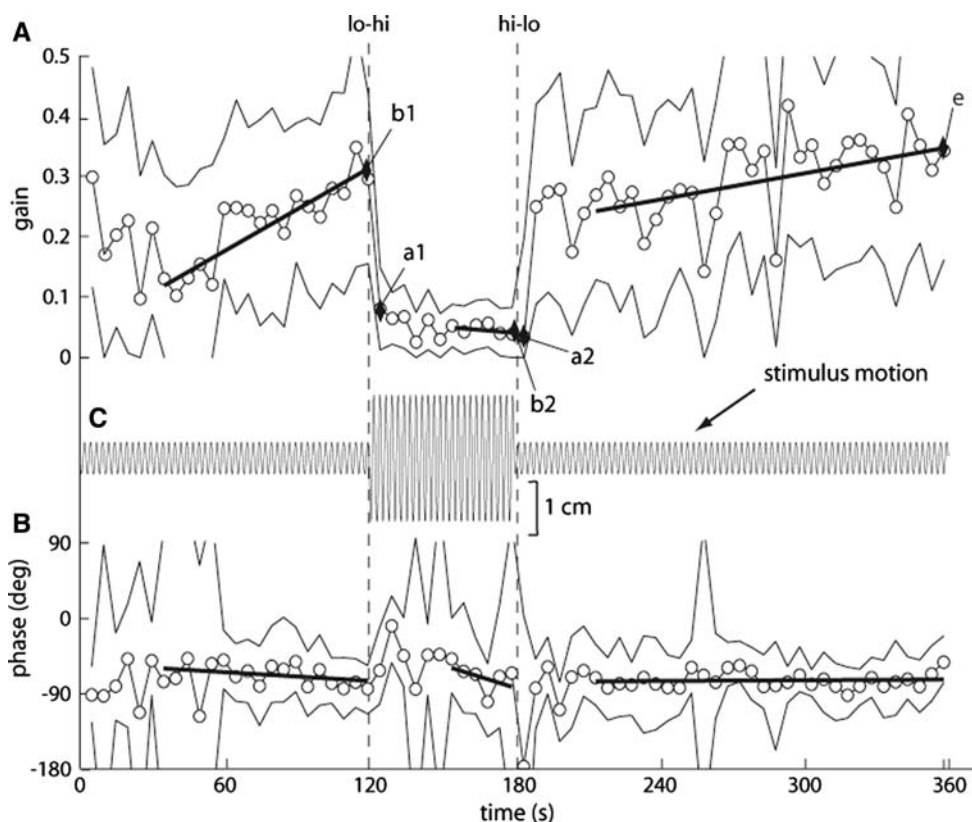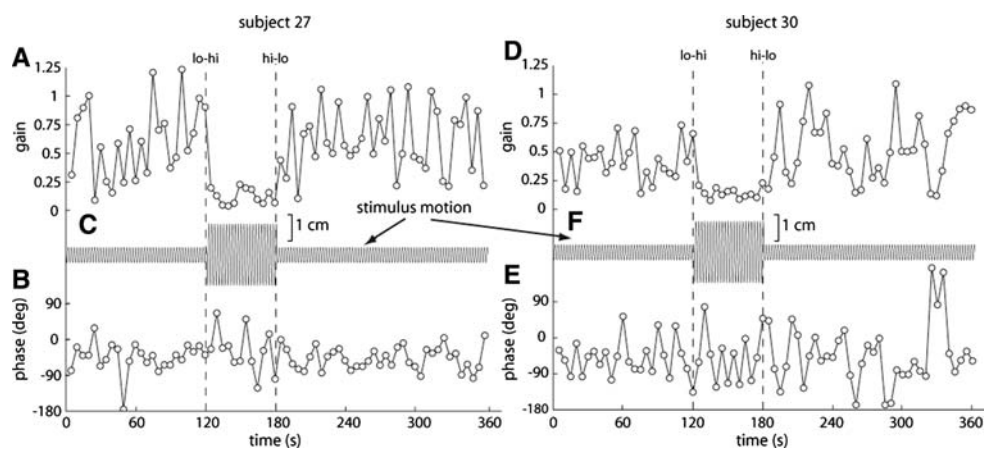

Fig. 5 Mean cycle-to-cycle (*A*) gain and (*B*) phase plotted with the (*C*) visual stimulus. Heavy black lines indicate gain and phase computed from the linear regression fits of FRFs over different time intervals. Gray lines indicate endpoints of conservative 95% confidence intervals (cf., Kiemel et al. 2006)

was high (e.g., Kiemel et al. 2006; Oie et al. 2002; Peterka 2002; Peterka and Benolken 1995; Mergner et al. 2003).

Some previous studies with visual motion as a stimulus have found that response amplitude (gain times stimulus amplitude) is roughly constant over some range of stimulus amplitudes (Peterka and Benolken 1995; Kiemel et al. 2006). Our data were not consistent with such "response saturation". For example, response amplitude during the high-amplitude stimulus in time interval $b2$ was 0.50 mm,

which was significantly less than the response amplitude during the low-amplitude stimulus in time intervals $b1$ (0.94 mm; unadjusted $p = 0.041$) and e (1.04 mm; unadjusted $p = 0.012$).

When visual motion amplitude was increased at 120 s or decreased at 180 s, the resultant change in the postural response differed. Gain of the averaged FRFs showed a significant difference ($p < 0.001$) between $b1$ and $a1$, when visual motion amplitude was increased, indicating a

significant decrease in gain within the first two cycles of stimulus motion. By contrast, no difference in gain ($p = 0.903$) was observed between intervals $b2$ and $a2$, indicating that gain of the averaged FRF did not increase significantly within the first two cycles of stimulus motion after the decrease in stimulus motion amplitude. No change in phase was detected between $b2$ and $a2$ ($p = 0.471$), though an increase in the variability of phase across subjects is observable at this change in stimulus motion amplitude.

Testing more explicitly for a temporal asymmetry, we tested whether the sum of the changes in FRFs at the two amplitude switches summed to zero (H_0: $(g_{b1} - g_{a1}) + (g_{b2} - g_{a2}) = 0$). Results revealed a significant difference from zero in the gain of the summed FRFs ($p = 0.007$), indicating that the observed changes in gain during the initial 5 s (two stimulus cycles) were significantly larger (i.e., faster) when stimulus motion increased versus when it decreased. If the FRF of interval $a2$ is replaced by the FRF of the next 5-s time interval, the contrast H_0 is no longer significantly different than zero (unadjusted $p = 0.75$), indicating that the amount of down-weighting that occurred within the first 5 s was similar to the amount of up-weighting that occurred within 10 s. In this sense, our data are consistent with down-weighting being about twice as fast as up-weighting.

Residual sway variability

Figure 6 shows how both position (Fig. 6a) and velocity (Fig. 6b) variability showed a significant increase when stimulus motion amplitude was increased at 120 s (p's < 0.002). After stimulus motion amplitude decreased back to low amplitude at 180 s, rather than decreasing to the level observed before 120 s, both position and velocity variability remained significantly higher (p's < 0.047) than during the initial portion of the trial (0–120 s), except that position variability was not different from the 60–120 s interval for the two intervals between 180 and 300 s (p's $= 0.055$).

Discussion

Sensory re-weighting as an adaptive process in the nervous system is not unique to the control of upright stance. Hypotheses of sensory re-weighting appear across many functional behaviors, including object perception and manipulation (Ernst and Banks 2002), perception of full-body motion (Lambrey and Berthoz 2003), and goal-directed reaching (Sober and Sabes 2003, 2005). However, few studies have investigated the dynamics of the re-weighting process. Here we studied the time course of sensory re-weighting and found evidence of a temporal
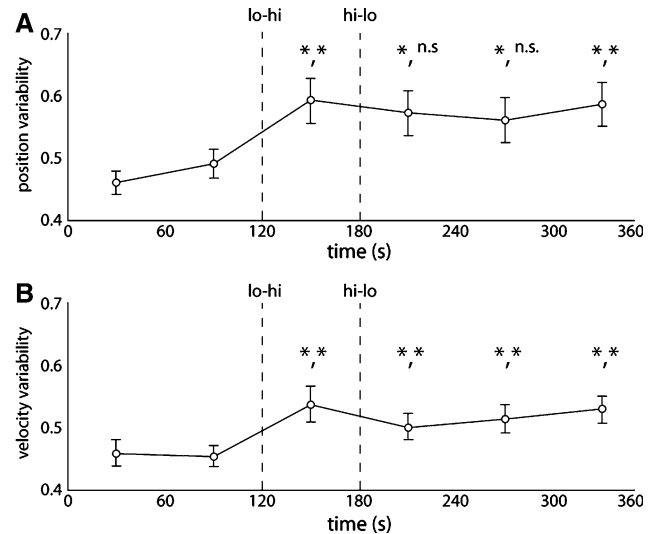

Fig. 6 Mean position and velocity variability averaged across subjects over 60 s intervals. *Error bars* indicate standard errors. *Asterisks* indicate significant differences between observed position or velocity variability in a given interval compared to the two intervals between 0–60 and 60–120, respectively

asymmetry that is qualitatively consistent with the predictions of an adaptive model (Carver et al. 2005, 2006). Specifically, when visual motion increased, gain decreased within 5 s to a value near to its asymptotic value. In contrast, when visual motion decreased, it took an additional 5 s for gain to increase by a similar absolute amount.

We emphasize that these values are general indications of the time scale of reweighting and should not be strictly viewed as time constants. Moreover, because our temporal resolution was limited to 5 s, the down-weighting time could be considerably faster than 5 s. Temporal resolution was limited by the trade-off with spatial resolution; we averaged responses across two stimulus periods to increase the accuracy of gain estimates.

In addition to the speed of re-weighting, it is noteworthy that we observed a temporal asymmetry that is consistent with the Carver et al. (2006) model. The model contains an adaptive Kalman filter that uses noisy sensory measurements to estimate the body's position and velocity (see Introduction). The relative weighting of visual and non-visual inputs in the Kalman filter is specified by an adaptive parameter, q, which is continually adjusted to minimize a performance index J, the mean squared ankle torque specified by the neural controller. (This choice of J is not crucial; there are other choices that lead to qualitatively similar behavior.) J is minimized by changing q at a rate proportional to $-dJ/dq$ (gradient descent).

The model's adaptive scheme leads to a temporal asymmetry qualitatively like that reported here (Carver et al. 2006). When motion of the visual scene is small, adaptation leads to substantial weighting of both visual and

non-visual inputs, since using all the available sensory information reduces the effect of sensory noise on sway and thus, the need for corrective ankle torques. When visual motion amplitude suddenly increases, the sway at the stimulus frequency suddenly increases, leading to a large increase in corrective ankle torques that are highly sensitive to changes in the adaptive parameter. As a result, the adaptive parameter changes quickly to down-weight vision and gain quickly decreases. Later, when visual motion amplitude suddenly decreases, there is only a small decrease in sway at the stimulus frequency, since gain is initially low. This small decrease in sway leads to a small decrease in corrective torques that is not very sensitive to changes in the adaptive parameter. As a result, the adaptive parameter changes slowly to up-weight vision and gain slowly increases. As noted above, when visual scene motion is small, substantial weighting of both visual and non-visual inputs reduces corrective ankle torques. Therefore, gain eventually increases to its original value.

The preceding description of the model's temporal asymmetry refers to the initial change in gain after a change in visual motion amplitude. In the model, the change in gain produced by a sudden change in visual motion amplitude is not exponential and therefore, cannot be characterized by a single fixed time constant. Changes in gain are only predicted to be approximately exponential for small changes in visual motion amplitude. Even with this approximation, the time constant depends on the current gain level. When gain is high, the time constant is small (fast); when gain is low the time constant is large (slow). This means that the time constant depends on the current gain level, not the direction in which gain is changing. For example, if visual motion amplitude is low and suddenly changed by a small amount, the model predicts that gain will quickly converge to a new level regardless of whether amplitude is increased or decreased.

While the behavior of gain was qualitatively consistent with the Carver et al. (2005) model, the sway variability results were only partially consistent. The model predicts the observed increase in sway variability as vision is down-weighted (120–180 s, see Fig 5). However, the predicted decrease in sway variability as vision is up-weighted (180–240 s, Fig 5) was not observed. The latter result is also not consistent with previous studies which found a consistent trade-off between re-weighting and variability (Allison et al. 2006). This trade-off reflects the degree of weighting to a stimulus versus the precision of estimating body dynamics. Large amplitude sensory inputs are down-weighted to minimize responses that would threaten stability, if for example, coupling to vision remained high. However, the consequence of down-weighting vision is reduced sensory information available for estimation, leading to increased sway variability at frequencies other

than the drive. Conversely, it is advantageous to up-weight small amplitude sensory inputs because more information is available for estimation, leading to a reduction in sway variability. Strong coupling to small amplitude inputs does not threaten stability. While this scenario has been supported in previous studies in which gain and sway variability was averaged over 2–4 min trials with constant-amplitude sensory stimuli (Allison et al. 2006), the dynamic measures used here indicate that overall stability does not behave similarly when the visual stimulus changes abruptly.

De Ruyter van Steveninck et al. have also shown evidence for sensory re-weighting at the level of neural coding (Brenner et al. 2000; Fairhall et al. 2001). The authors presented evidence of adaptive scaling of the transfer function of motion-sensitive neurons in the fly visual system based upon the variance of the visual input, such that information is optimized across a wide range of sensory contexts, as well as a temporal asymmetry dependent upon whether variance increased or decreased. Adaptation of the sort demonstrated by Brenner et al. (2000) and Fairhall et al. (2001), as well as in the current study, where adaptation is based upon a statistical property of the sensory input, necessitates that the nervous system estimates these statistics, at least implicitly. Taken from this context, and as pointed out by Tin and Poon (2005), these related concepts of estimation, adaptive control and internal models have been influential in furthering our understanding of processes of sensorimotor integration, and by extension, multisensory integration. The present empirical results add to our understanding of adaptive processing by demonstrating that the temporal asymmetry observed in sensory re-weighting dynamics may be a general property of adaptive estimation in the nervous system.

Conclusion: a functional interpretation

The observed temporal asymmetry in sensory re-weighting can also be evaluated from a functional perspective: Upright stance is inherently unstable, and the stance control system must continuously respond to internal and external perturbations that could produce an injurious fall. The current thinking is that this response must be fast to be beneficial. The present results suggest that in the case of up-weighting to a stimulus, a slow process may be preferable. In our paradigm, when visual motion amplitude is low, vision provides a relatively stable source of information for stance control. When visual motion amplitude is increased beyond the stability boundaries of upright stance, visual information provides a poor source of information for stance control. Under such conditions, if gain to visual motion remains high, the large visual motion amplitude threatens balance, and the stance control system must

diminish the visual weighting rapidly in order to maintain upright standing. On the other hand, if current visual motion amplitude is large and stance is already stable, decreasing visual motion amplitude does not threaten balance and adapting rapidly to the new sensory conditions is not critical to avoid falling. One may argue that slow up-weighting reflects a conservative CNS strategy. Rapid up-weighting may cause instability if the change in sensory conditions is transient. Slow up-weighting insures stronger coupling to only sustained changes in the sensory surround. Thus, the temporal asymmetry can be interpreted to reflect a scheme in which the nervous system commits resources to sensory re-weighting based upon a functional need. Balance control entails an inherent "cost function", minimizing fall-risk, which modulates adaptive processes such as sensory re-weighting, suggestive of a cognitive component to the re-weighting process.

Appendix

In this study we used gain computed in successive 5-s intervals to track changes in the coupling strength of postural sway to visual motion (see Methods). However, this method is potentially subject to biases due to transient sway responses and side-lobe leakage of power from non-stimulus frequencies. Our particular concern was that these errors might be systematically different during up- and down-weighting, leading to an apparent temporal asymmetry that does not reflect a true temporal asymmetry in coupling strength to the stimulus. Here we describe simulations that show that: (1) biases due to transients, although present, are too small to explain the temporal asymmetry observed in our data; and (2) side-lobe leakage does not bias FRF values, consistent with the assumptions of our statistical analysis.

To assess the biases due to transient responses and side-lobe leakage we needed a quantitative stochastic model of how the body's center of mass responds to motion of the visual scene. We used a linear stochastic model from a previous study (Kiemel at al. 2006) combined with various hypothesized time courses of coupling strength changes. The linear stochastic model is $\dot{x}(t) = Ax(t) + B\xi(t) + Cu(t - \tau)$, where t is time, $u(t)$ is the position of the visual scene, $x(t)$ is a 5-by-1 vector whose first component is the

body's center of mass, $\xi(t)$ is white noise, A is a 5-by-5 matrix, B and C are 5-by-1 vectors, and τ is a time delay. In Kiemel et al. (2006), A, B, C and τ were fit based on data from individual subjects and conditions. We used the parameters from subject 1 in the low-amplitude condition. Parameters from other subjects and conditions would produce similar results. We modified the model by scaling the noise level by a factor β and adding a changing coupling strength $\alpha(t)$: $\dot{x}(t) = Ax(t) + \beta B\xi(t) + \alpha(t)Cu(t - \tau)$.

We simulated the model using the visual scene motion $u(t)$ from our experimental protocol. We assumed that coupling strength $\alpha(t)$ had different asymptotic values for each amplitude of visual motion. These asymptotic values were chosen to reproduce our empirical estimates of group gain during time intervals $b1$ and $b2$ (see Fig. 5). As a simplification (see Discussion), we assumed that after a switch in visual motion amplitude, $\alpha(t)$ decayed exponentially with time constant τ_α to its new asymptotic value. We ran simulations with various values of τ_α. For each simulation, we computed gain before each switch, g_{b1} and g_{b2}, and during the 5-s interval after each switch, g_{a1} and g_{a2}, using the same method applied to our experimental data.

To assess biases due to transients, we first simulated the model without noise ($\beta = 0$). Figure 7a shows the absolute initial gain change during down-weighting, $g_{b1} - g_{a1}$, and during up-weighting, $g_{a2} - g_{b2}$, as a function of the time constant τ_α. To assess how accurately these initial gain changes reflect the underlying initial change in coupling strength $\alpha(t)$, we averaged $\alpha(t)$ in the 5-s interval following each switch and computed the model's corresponding steady-state gain. The magnitude of the resulting "underlying" initial gain change, which is the same for both down- and up-weighting, is shown as the grey curve in Fig. 7a. Note that measured gain changes are fairly close to the "underlying" gain change, indicating that the measured changes in gain are a reasonable reflection of the change in coupling strength. Importantly, gain changes measured during down- and up-weighting for the same time constant τ_α were very similar.

To assess biases due to side-lobe leakage, we simulated the model with noise ($\beta > 0$). Figure 7b shows the FRF value in time interval b1 from 30 simulations. Note that Fig. 7b is similar to Fig. 2a, although the variation in Fig. 7b is due solely to sampling errors, whereas the variation in Fig. 2a is due to both sampling errors and subject differences. Sampling errors for the model are due to side-lobe leakage of power from non-stimulus frequencies. Side-lobe leakage does not bias the FRF value in the complex plane; the mean FRF from the 30 simulations (closed circle) is not significantly different than the FRF value computed without noise (open circle). In contrast, the mean gain from the 30 simulations (absolute value of open square) does exhibit a positive bias compared to the gain
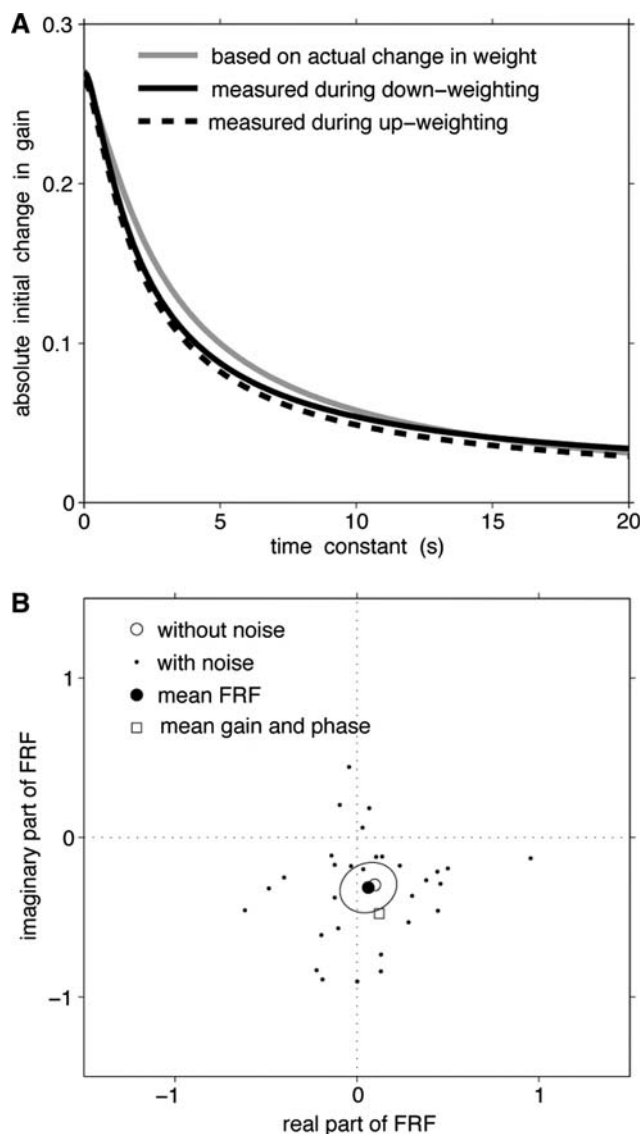
Fig. 7 Analysis method applied to simulated data. **a** Initial change in gain for simulated data without noise. **b** FRF values for time interval b1 for simulation without noise (*open circle*) and 30 simulations with noise (*dots*). The *closed circle* indicates the mean FRF for the 30 simulations. The *open square* indicates an FRF value whose absolute value and argument are the mean gain and circular mean phase for the 30 simulations. See text for further explanation

computed without noise (absolute value of open circle). Thus, side-lobe leakage biases gain values but not FRF values. Since our statistical analysis is based on the distribution of FRF values, side-lobe leakage does not bias our statistical results.

References

Allison L, Kiemel T, Jeka JJ (2005) The dynamics of multisensory reweighting in healthy and fall-prone older adults. 35th annual meeting of the Society for Neuroscience, Washington DC

Allison L, Kiemel T, Jeka JJ (2006) Multisensory reweighting is intact in healthy and fall-prone older adults. Exp Brain Res 175(2):342–352

Anastasio T, Patton P (2004) Analysis and modeling of multisensory enhancement in the deep superior colliculus. In: Calvert G, Spence C, Stein BE (eds) Handbook of multisensory processes. MIT Press, Boston

Bendat JS, Piersol AG (2000) Random Data: Analysis & Measurement Procedures. Wiley-Interscience, New York

Brenner N, Bialek W, van Stevenink R (2000) Adaptive rescaling maximizes information transmission. Neuron 26:695–702

Bronstein AM, Hood JD, Gresty MA, Panagi C (1990) Visual control of balance in cerebellar and Parkinsonian syndromes. Brain 113:767–779

Carver S, Kiemel T, van der Kooij H, Jeka JJ (2005) Comparing internal models of the dynamics of the visual environment. Biol Cybern 92(3):147–163

Carver S, Kiemel T, Jeka JJ (2006) Modeling the dynamics of sensory reweighting. Biol Cybern 95(2):123–134

Dijkstra TMH, Schöner G, Giese MA, Gielen CCAM (1994) Frequency dependence of the action-perception cycle for postural control in a moving visual environment: relative phase dynamics. Biol Cybern 71:489–501

Ernst MO, Banks MS (2002) Humans integrate visual and haptic information in a statistically optimal fashion. Nature 415:429–433

Fairhall AL, Lewen GD, Bialek W, van Stevenink R (2001) Efficiency and ambiguity in an adaptive neural code. Nature 412:787–792

Hay L, Bard C, Fleury M, Teasdale N (1996) Availability of visual and proprioceptive afferent messages and postural control in elderly adults. Exp Brain Res 108:129–139

Hochberg Y, Tamhane AC (1987) Multiple comparison procedures. Wiley, New York

Horak FB, Macpherson JM (1996) Postural orientation and equilibrium. In: Shepard J, Rowell L (eds) Handbook of physiology. Oxford University Press, New York, pp 255–292

Jeka JJ, Oie KS, Schöner G, Dijkstra TMH, Henson EM (1998) Position and velocity coupling of postural sway to somatosensory drive. J Neurophys 79:1661–1674

Jeka JJ, Oie KS, Kiemel T (2000) Multisensory information for human postural control: integrating touch and vision. Exp Brain Res 134:107–125

Keshner EA, Kenyon RV, Langston J (2004) Postural responses exhibit Multisensory dependencies with discordant visual and support surface motion. J Vestib Res 14:307–319

Kiemel T, Oie KS, Jeka JJ (2002) Multisensory fusion and the stochastic structure of postural sway. Biol Cybern 87:262–277

Kiemel T, Oie KS, Jeka JJ (2006) Slow dynamics of postural sway are in the feedback loop. J Neurophys 95:1410–1418

Knill D, Pouget A (2004) The Bayesian brain: the role of uncertainty in neural coding and computation. Trends Neurosci 27(12):712–719

Kuo AD (2005) An optimal state estimation model of sensory integration in human postural balance. J Neural Eng 2(3):S235–S249

Lambrey S, Berthoz A (2003) Combination of conflicting visual and non-visual information for estimating actively performed body turns in virtual reality. Int J Psychophysiol 50:101–115

Mahboobin A, Loughlin PJ, Redfern MS, Sparto PJ (2005) Sensory re-weighting in human postural control during moving-scene perturbations. Exp Brain Res 167(2):260–267

Mergner T, Maurer C, Peterka RJ (2003) A multisensory posture control model of human upright stance. Prog Brain Res 142:189–201

Oie KS, Kiemel T, Jeka JJ (2001) Human multisensory fusion of vision and touch: detecting nonlinearity with small changes in the sensory environment. Neurosci Lett 315:113–116

Oie KS, Kiemel T, Jeka JJ (2002) Multisensory fusion: simultaneous re-weighting of vision and touch for the control of human posture. Cog Brain Res 14:154–176

Oie K, Carver S, Kiemel T, Barela J, Jeka J (2005) The dynamics of sensory reweighting: a temporal asymmetry. Gait Posture 21(1):S29

Peterka RJ (2002) Sensorimotor integration in human postural control. J Neurophys 88(3):1097–1118

Peterka RJ, Benolken MS (1995) Role of somatosensory and vestibular cues in attenuating visually induced human postural sway. Exp Brain Res 105:101–110

Pouget A (2006) Neural basis of Bayes-optimal multisensory integration: theory and experiments. Computational and systems neuroscience 2006, Models of multisensory integration: psychophysical and neural contraints. Salt Lake City, UT

Seber GAF (1984) Multivariate observations. Wiley, New York

Sober SJ, Sabes PN (2003) Multisensory integration during motor planning. J. Neurosci 23(18):6982–6992

Sober SJ, Sabes PN (2005) Flexible strategies for sensory integration during motor planning. Nature Neurosci 8(4):490–497

Teasdale N, Stelmach GE, Breunig A (1991a) Postural sway characteristics of the elderly under normal and altered visual and support surface conditions. J.Gerontol. 46:B238–B244

Teasdale N, Stelmach GE, Breunig A, Meeuwsen HJ (1991b) Age differences in visual sensory integration. Exp Brain Res 85:691–696

Teasdale N, Bard C, LaRue J (1993) Fleury M On the cognitive penetrability of posture control. Exp Aging Res 19:1–13

Tin C, Poon CS (2005) Internal models in sensorimotor integration: perspectives from adaptive control theory. J Neural Eng 2:S147–S153

Todorov E (2004) Optimality principles in sensorimotor control. Nature Neurosci 7(9):907–915

van der Kooij H, Jacobs R, Koopman B, Grootenboer H (1999) A multisensory integration model of human stance control. Biol Cybern 80:299–308

van der Kooij H, Jacobs R, Koopman B, van der Helm F (2001) An adaptive model of sensory integration in a dynamic environment applied to human stance control. Biol Cybern 80:1211–1221

Winter DA (1991) Biomechanics and motor control of human movement, 2nd edn. Wiley-Interscience, New York

Wolpert DM, Ghahramani Z (2000) Computational principles of movement neuroscience. Nat Neurosci 3:1212–1217

Woollacott MH, Shumway-Cook A, Nashner LM (1986) Aging and posture control: changes in sensory organization and muscular coordination. Int J Aging Hum Dev 23(2):97–114